ANTIOXIDANTS & REDOX SIGNALING
Volume 7, Numbers 9 & 10, 2005

Forum Original Research Communication

Differentiated Alzheimer's Disease Transmitochondrial Cybrid Cell Lines Exhibit Reduced Organelle Movement

PATRICIA A. TRIMMER and M. KATHLEEN BORLAND

ABSTRACT

The axonal transport and function of organelles like mitochondria and lysosomes may be impaired and play an important role in the pathogenesis of Alzheimer's disease (AD). Unique cybrid cell lines that model AD pathology were created by fusing platelets containing mitochondria from age-matched AD and control volunteers with mitochondrial DNA-free SH-SY5Y human neuroblastoma cells. These cybrid lines were differentiated to form process-bearing neuronal cells. Mitochondria and lysosomes in the neurites of each cybrid line were fluorescently labeled to determine the kinetics of organelle movement. The mitochondria in AD cybrid neurites were elongate, whereas the mitochondria in control cybrid neurites were short and more punctate. The mean velocity of mitochondrial movement, as well as the percentage of moving mitochondria, was significantly reduced in AD cybrids. The velocity of lysosomal movement was also reduced in the processes of AD cybrid cells, suggesting that the axonal transport machinery may be compromised in cybrid cell lines that contain mitochondrial DNA derived from AD patients. Reduced mitochondrial and lysosomal movement in susceptible neurons may compromise function in metabolically demanding structures like synaptic terminals and participate in the terminal degeneration that is characteristic of AD. *Antioxid. Redox Signal.* 7, 1101–1109.

INTRODUCTION

CNS NEURONS are highly differentiated cells with elaborately branched dendritic arbors, as well as an axon that can extend for up to a meter in length. This polarized morphology makes neurons susceptible to disruption of cellular transport systems (13). Organelles like mitochondria and lysosomes are distributed to postsynaptic structures, including dendritic spines, by an active transport system. Anterograde axonal transport is responsible for the delivery of these and other synaptic components, such as choline acetyltransferase and amyloid precursor protein (APP), to axonal terminals (6, 40, 44). Retrograde transport delivers trophic factors like brain derived neurotrophic factor and nerve growth factor, as well as membrane bound organelles like mitochondria and lysosomes, to the cell body (21, 39).

The movement of organelles like mitochondria and lysosomes depends on the microtubule-based, ATP-binding motor proteins, including members of the kinesin family and cytoplasmic dynein, which move organelles anterograde and retrograde, respectively (5). Lysosomes are part of a dynamic system that maintains cell viability by recycling damaged or dysfunctional cellular constituents and protein aggregates (32). Lysosomes are up-regulated in Alzheimer's disease (AD) and this may represent a neuronal compensatory response against the accumulation of protein inclusions. Loss of lysosome transport in neurons could restrict this compensatory response and limit neuronal viability (3, 9). The distribution of mitochondria to distal axons, dendrites, and synaptic terminals is especially important because neurons require a local supply of ATP to support the generation of membrane potentials and buffer local changes in calcium concentration (34, 35). Changes in the distribution of mitochondria in neuronal processes are deleterious and can lead to altered process growth, terminal degeneration, and cell death (36). Altered axonal transport of essential cellular organelles and constituents could therefore

Department of Neurology, University of Virginia, Charlottesville, VA.

result in the loss of synapses by living neurons and ultimately neuronal cell death seen in AD (10, 34).

What evidence exists that altered axonal transport plays a role in AD pathogenesis? Dystrophic neurites in AD cortex biopsies have cytoskeletal and membrane abnormalities consistent with a disruption of axonal transport (8, 43). AD brain is also characterized by a progressive loss of synaptic vesicle protein expression (33). Dai *et al*. (14) recently visualized a decrease in temporal cortex axonal transport in AD brain tissue by using a postmortem tracing method. The results of these studies suggest that a disruption in axonal transport may play a critical role in the neuronal dysfunction seen in AD.

Numerous studies have shown that human disease can be caused by defects in mitochondrial DNA (mtDNA) that result in compromised mitochondrial function. Impaired mitochondrial function, especially at the level of the electron transport chain (ETC), may play a key role in the pathogenesis of AD (49). Specific decreases in cytochrome *c* oxidase (CO) activity, complex IV in the mitochondrial ETC, have been detected in the brain tissue and platelets of AD patients (for review, see 49). AD brain tissue harbors mtDNA mutations that could account for the decrease in oxidative phosphorylation seen in AD (12). Mitochondrial dysfunction in AD has also been associated with increased levels of oxidative stress and altered calcium homeostasis (34, 42). Finally, morphologically abnormal mitochondria have been found in neurons and synapses of AD brains (18, 45).

Cytoplasmic hybrid ("cybrid") cell models have been used to demonstrate the role dysfunctional mitochondria play in the pathogenesis of AD (25, 50). Cybrid cells were created by introducing mitochondrial genes from the platelets of sporadic AD patients or symptom-free, age-matched control (CNT) volunteers into human, SH-SY5Y neuroblastoma cells that have been depleted of endogenous mtDNA (ρ° cells). The ρ° cells were generated by prolonged incubation in low concentrations of ethidium bromide (38). Platelets exhibit abnormalities in calcium regulation and oxidative metabolism and have been widely used to study AD (15, 22). Platelets also express APP, accumulate β-amyloid (Aβ) isoforms, and exhibit a decrease in CO activity that is comparable to the decrease seen in AD brain tissue (15,41). Removal of metabolic support following cybrid fusion selects cybrid cell lines that are adequately repopulated with platelet mitochondria and are capable of sustaining oxidative phosphorylation. Multiple replication cycles yield cybrid cell lines with constant environmental and nuclear genetic backgrounds that differ from each other only in the source of their mitochondrial genes (38, 49).

Cybrid cell lines that have been repopulated with mtDNA from AD platelets exhibit disruption of many vital cell functions that recapitulate changes seen in AD brain. For example, AD cybrid cell lines have increased levels of reactive oxygen species (ROS) and free radical-scavenging enzymes (50), altered intracellular calcium signaling with reduced mitochondrial calcium stores (46), increased numbers of enlarged, disrupted mitochondria (52), and reduced mitochondrial membrane potential that can be partially restored by antioxidant treatment (7, 24). AD cybrid cells oversecrete Aβ peptides, have increased cellular Aβ peptide levels, and accumulate Congo red-positive amyloid deposits in culture (24). The chronic changes in bioenergetic functions typical of AD cybrid cell lines are reproducible (53). Furthermore, direct comparison of mitochondrial morphology and function in low (p = 8–10) and high (p = 14–16) passage AD and CNT cybrid cell lines showed that there is a phenotypic drift toward increased mitochondrial dysfunction, in part because defective mitochondrial genes exhibit a replicative advantage (53). Our results thus far firmly establish cybrid cell lines as important tools that can be used to understand sporadic AD, in terms of both abnormal cell physiology and production of characteristic cytopathology.

AD and CNT cybrids can also be differentiated into process-bearing neuronal cells using chemically defined medium and retinoic acid (26). Differentiated AD cybrids provide a model of a process-bearing neuron harboring persisting bioenegetic defects in mitochondrial ETC function. In this study, we visualized mitochondria and lysosomes in the processes of differentiated AD and CNT (dAD and dCNT) cybrid cell lines to determine if the ETC defect in AD cybrids alters the kinetics of mitochondrial and lysosomal axonal transport. Our results firmly establish that the velocity of mitochondrial and lysosomal movement in the processes of AD cybrid cell lines is significantly reduced. These results further suggest that chronic mitochondrial dysfunction can lead to compromise of the axonal transport system in AD neurons.

MATERIALS AND METHODS

AD and CNT cybrid cell lines were created, and characterized as previously described (50). All cell lines were retrieved from frozen stocks as matched sets so that cells were grown for comparable periods of time (equivalent numbers of passages) in culture prior to differentiation. New stocks of all replicating cybrid lines were retrieved from frozen stocks every 2 months to avoid mycoplasma contamination. Replicating, undifferentiated cybrid cell lines were maintained in serum-containing culture medium as previously described (52). To differentiate AD and CNT cybrid cell lines, the cells were plated at low density into poly-L-lysine-coated coverslip culture dishes (MatTek, Ashland, MA, U.S.A.) and incubated in 10 μ*M trans*-retinoic acid (Calbiochem, La Jolla, CA, U.S.A.) in serum-containing culture medium. After 7–10 days, the serum-containing culture medium was replaced with a defined medium consisting of Dulbecco's modified Eagle's medium (high glucose), N2 supplement, 1% ovalbumin, sodium pyruvate (100 μg/ml), 0.5 mg/ml uridine, penicillin (100 IU/ml), and streptomycin (50 μg/ml). All medium components except serum were from Invitrogen (Grand Island, NY, U.S.A.). Movement was measured in differentiated cybrid cells after 14–21 days following the beginning of the differentiation procedure.

To measure mitochondrial movement, dAD and dCNT cells were incubated with 50 n*M* MitoTracker CMXRos (MTRed; Molecular Probes, Eugene, OR, U.S.A.) for 10 min at 37°C. dAD and dCNT cybrid cells were incubated with 200 n*M* LysoTracker Red DND-99 (LysoRed; Molecular Probes) for 1 h to visualize lysosomes. Time-lapse recordings of labeled mitochondrial and lysosomal movement were made on an Olympus IX70 microscope equipped with epifluoresence and Nomarski optics, a Lambda 10–2 filter wheel (Sutter Instruments, Novato, CA, U.S.A.), a MicroMax Princeton Instruments digital camera (Roper Scientific, Trenton, NJ, U.S.A.)

and a heater/controller (World Precision Instruments, Inc., Sarasota, FL, U.S.A.) to maintain cybrid cells at 37°C during image collection. Collection of image stacks and velocity measurements were made using the MetaMorph Imaging System (Universal Imaging Corp., Downingtown, PA, U.S.A.). For standard recordings, images of the organelles in one neurite per cybrid cell were collected every 3 s for 2 min. Unlike other studies, the velocity of all mitochondria or lysosomes in each cybrid process was determined whether they moved or not (28, 29). The run length (distance traveled without stopping), total excursion length (total distance traveled irrespective of direction during the recording period), average velocity, percent not moving, and percent of time spent moving were all determined. The tip-to-tip length of each mitochondrion was also measured. Neutral density filters were used to reduce illumination from the mercury lamp. Exposure periods (30–50 ms) were kept at a minimum to limit phototoxicity. For each study, dCNT cells were imaged first to establish optimal conditions.

Mitochondria and lysosomes in each frame of every video recording were individually tracked using the MetaMorph Imaging System. The average velocity was calculated for each organelle during the 3-min recording period. Then the average velocity of every mitochondrion or lysosome in each cybrid neurite (one neurite measured per cell) was averaged to obtain the average velocity for mitochondrial or lysosomal movement per neurite. The average organelle velocity per neurite was used to generate the data shown in Table 1. The data were analyzed using Statistica software (StatSoft, Tulsa, OK, U.S.A.) and Excel (Microsoft, Redmond, WA, U.S.A.) *t* test assuming equal or unequal variance.

AD subjects met the National Institute of Neurological and Communicative Disorders and Stroke and Alzheimer's Diseases and Related Disorders Association (NINCDS-ADRDA) criteria for probable AD. Individuals in the AD group did not have indications of any other neurodegenerative diseases, including familial AD. CNT subjects were cognitively normal, age-matched, and sex-matched to AD subjects. All AD and CNT subjects were recruited after Institutional Review Board approval as previously described (52).

RESULTS

Subject data

The six CNT and eight AD cybrid lines used to study mitochondrial movement were derived from a larger group of age-matched (range 55–79, mean age for AD = 69.6 years; range 49–67, mean age for CNT = 60.2 years) cybrid lines (52). There were three females and three males in the CNT group and five females and three males in the AD group. A smaller subset of three CNT and three AD cybrid lines was used to assess changes in lysosome movement. CO activity was measured in samples of AD and CNT cybrid lines at low passage (see 53). CO activity in this subset of AD cybrid cell lines was not statistically different from that in CNT, although significance was achieved in larger studies of AD and CNT cybrid cell lines generated by our research group (52; see 50 for method). In CNT cybrids, CO activity ranged from 0.0122 to 0.0547 n*M*/s/mg (average = 0.0342). CO activity in the AD cybrids ranged from 0.0139 to 0.0752 n*M*/s/mg (average = 0.0293).

Mitochondrial morphology and movement in differentiated cybrid neurites

In cybrid neurites of comparable length (data not shown) stained with MTRed, the mitochondria in dAD neurites were long and thread-like, whereas mitochondria in dCNT neurites were shorter and more punctate (Fig. 1). The number of mitochondria in dAD cybrid processes ranged from four to 19, whereas the number of mitochondria in dCNT cybrid processes

Table 1. Summary of Measurements of Mitochondrial and Lysosomal Velocity

	AD	*CNT*
Mitochondria	*n* = 69 neurites	*n* = 51 neurites
Average velocity* (μm/s)	0.075 ± 0.0037	0.106 ± 0.0054
Percent not moving†	68.36%	51.75%
Total excursion length* (μm)	4.8 ± 0.308	6.74 ± 0.471
Time moving* (s)	53.72 ± 0.913	58.56 ± 1.14
Run length* (μm)	0.72 ± 0.109	1.6 ± 0.207
Mitochondrial length† (μm)	4.61 ± 0.31	3.35 ± 0.269
Lysosomes	*n* = 31 neurites	*n* = 15 neurites
Average velocity‡ (μm/s)	0.105 ± 0.014	0.141 ± 0.0054
Total excursion length* (μm)	10.71 ± 0.501	14.53 ± 0.542
Time moving† (s)	89.57 ± 1.64	109.24 ± 0.866

The table summarizes the measurements of mitochondrial and lysosomal velocity determined in this study. The mitochondrial data were collected from 69 processes derived from individual cells in eight AD cybrid lines that contained from four to 19 mitochondria per process. The CNT mitochondrial data were collected from 51 processes of individual cells in six cybrid lines that contained from seven to 28 mitochondria per process. The lysosome data were collected from three AD and three CNT cybrid lines. The 15 CNT processes analyzed contained two to 24 lysosomes per process, whereas the 31 AD cybrid processes contained three to 21 mitochondria per process. Data are given as means ± SEM.

*Significant at $p < 0.001$ using a *t* test assuming equal or unequal variance.

†Significant at $p < 0.05$ using a *t* test assuming equal or unequal variance.

‡Significant at $p < 0.001$ using a *t* test assuming equal variance.

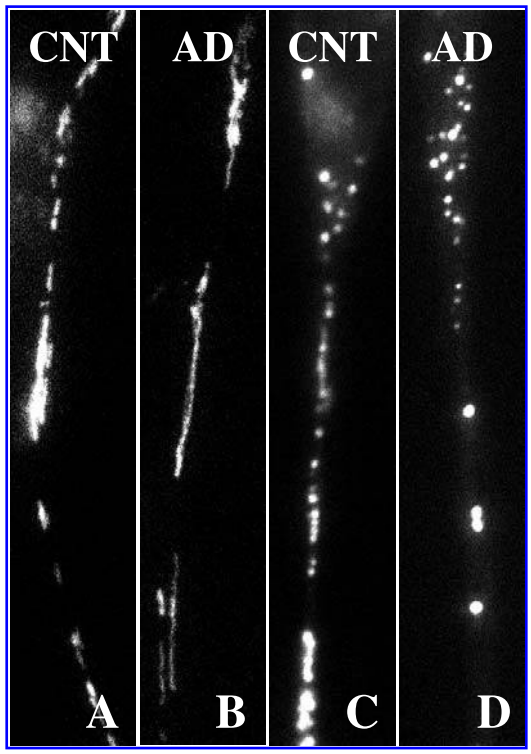

FIG. 1. Mitochondria and lysosomes in dAD and dCNT cybrid neurites were stained with MTRed and LysoRed, respectively. (**A** and **B**) The morphology of mitochondria in the neurites from dCNT and dAD cybrid cells. The mitochondria in the dAD cybrid neurite were longer and more thread-like. (**C** and **D**) The morphology of lysosomes in the neurites of dCNT and dAD cybrid cells.

ranged from seven to 28. Quantitative measurements subsequently confirmed that the mitochondria in dAD cybrid neurites were significantly longer than mitochondria in dCNT neurites (Table 1). The length of each mitochondrion found in 72 different cell processes in seven dAD cybrid cell lines was significantly different ($p < 0.05$) from the mitochondrial length in 49 different cell processes in six dCNT cybrid cell lines using a dependent *t* test (Table 1). In general, the total mass of all the mitochondria in each cybrid neurite was equivalent, although the number of mitochondria varied (data not shown). When mitochondrial length and velocity were correlated for all the mitochondria tracked in one dAD and one dCNT cybrid cell line (Fig. 2), the longer, thread-like dAD mitochondria were also slower than the shorter dCNT mitochondria.

Mitochondrial movement was bidirectional and saltatory, that is, characterized by frequent starts and stops. Even in CNT cell processes, a substantial percentage of mitochondria were stationary for a portion of the recording period (Table 1, percent not moving). A histogram of the average velocity of mitochondrial movement was created for dAD and dCNT cybrids and is shown in Fig. 3. The mitochondria in 69 different dAD cybrid neurites moved at a significantly reduced velocity ($p \leq 0.001$) when compared with mitochondria in neurites from 51 different dCNT cells using a *t* test for samples assuming equal or unequal variance (Table 1). A two-sample *F* test was used to analyze the variance and standard deviation of the mean mitochondrial velocities per process for each dAD and dCNT cybrid line. The range in variance for the dAD cybrid lines (0.0003–0.0143, mean 0.0055) was not significantly different from the range in the variance in the processes of dCNT cybrid lines (0.0055–0.0164, mean 0.0118). The mean mitochondrial velocity calculated for the seven dAD cybrid lines was 0.075 μm/s with a standard deviation of 0.016 and a standard error (SEM) of 0.0037. The mean mitochondrial velocity for the six dCNT cell lines was 0.106 μm/s with a standard deviation of 0.020 and a SEM of 0.0054. The mean AD and CNT mitochondrial velocities were significantly different using a *t* test assuming either equal or unequal variance at $p \leq 0.01$ (two-tail).

The decreased velocity of mitochondrial movement is due, in part, to a significant increase in the percentage of mitochondria that fail to achieve a minimum velocity of 0.05 μm/s (Table 1, percent not moving), a reduction in the total excursion length (total distance mitochondria traveled during the recording period in 69 dAD and 39 dCNT cybrid neurites), time

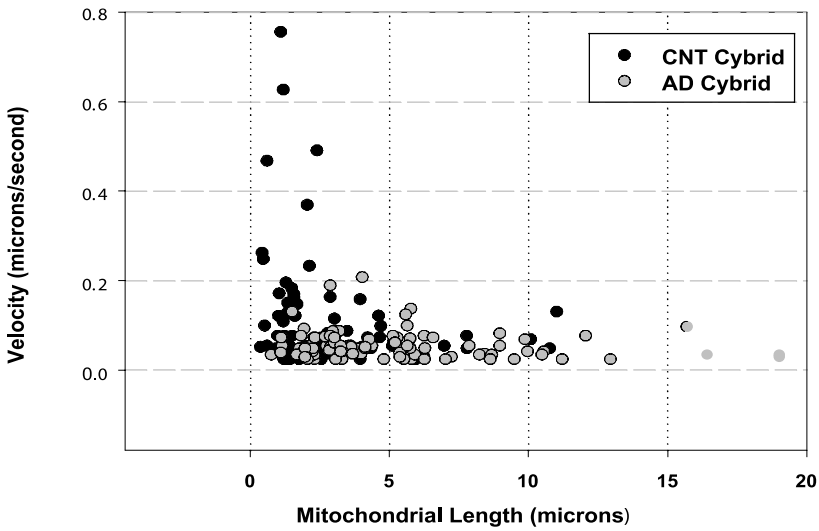

FIG. 2. This scatterplot shows the paired length and velocity of all mitochondria ($n = 96$) in seven neurites from one dAD cybrid cell line (gray circles). The mitochondria in this typical dAD cybrid line were longer and moved more slowly than the mitochondria ($n = 89$) in eight neurites of one typical dCNT cybrid cell line (black circles).

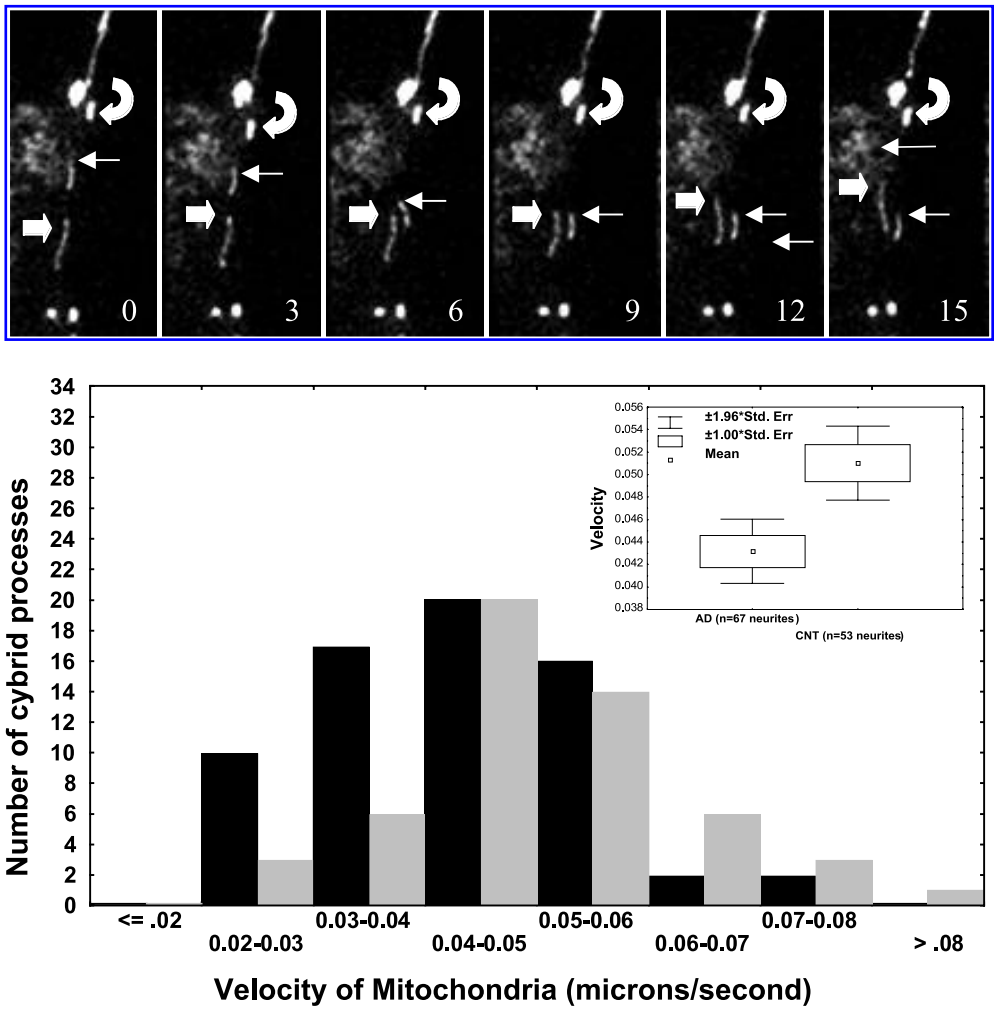

FIG. 3. This montage shows images of MTRed-labeled mitochondria in a dCNT neurite taken every 3 s (elapsed seconds shown on each image). The mitochondrion indicated by the wide arrow moved in a retrograde direction. Diffuse staining near the wide arrow is derived from labeled mitochondria in the cell in another focal plane. The mitochondrion indicated by the straight thin arrow moved anterograde during the recording period. The mitochondrion indicated by the curved arrow showed minimal movement during the recording period. The histogram shows that the mean velocity of mitochondrial movement in the processes of 69 dAD cybrid cell processes (black bars) was significantly reduced ($p < 0.01$) when compared with movement of mitochondria in the processes of 51 dCNT cybrid cell processes (gray bars) using both the *t* test for dependent samples and the Wilcoxon matched pairs test. The same data are shown in the bar and whisker chart (**inset**).

spent moving (based on 566 dAD and 548 dCNT mitochondria), and run length (distance traveled between stops) of 544 dAD and 614 dCNT mitochondria in cybrid neurites (Table 1). Nevertheless, some mitochondria in both dAD and dCNT cybrid neurites achieved maximum velocities of 1–2.6 μm/s.

Figure 3 includes a montage of images that illustrate the movement of three mitochondria in a differentiated cybrid neurite. Few mitochondria moved retrograde even in dCNT cybrid neurites. Consequently, the number was not sufficient to allow us to determine if anterograde and retrograde movements were differentially affected in dAD cybrids.

Lysosomal morphology and movement in differentiated cybrid neurites

The LysoRed-stained lysosomes in dAD and dCNT cybrid neurites of comparable length (data not shown) were spherical in shape and ranged in diameter from 0.52 to 0.94 μm. The lysosomes in dAD and dCNT cybrid neurites were comparable in diameter and shape (Fig. 1). The number of lysosomes ranged from three to 24 in dAD cybrid neurites and three to 21 in dCNT cybrid neurites. In dCNT cells, lysosomes moved consistently either anterograde or retrograde with far fewer changes in direction than mitochondria. Only a small percentage of the lysosomes remained stationary during the recording period (data not shown). Lysosomes in dAD cybrid neurites did not travel as far (total excursion length) and also spent less time moving during the recording period than dCNT lysosomes. A histogram of the average velocity of lysosomal movement was created for dAD and dCNT cybrids and is shown in Fig. 4. The lysosomes in 31 different dAD cybrid neurites moved at a significantly reduced velocity ($p < 0.001$) using a *t* test assuming equal variance when compared with lysosomes in the neurites of 15 different dCNT cybrid neurites (Table 1).

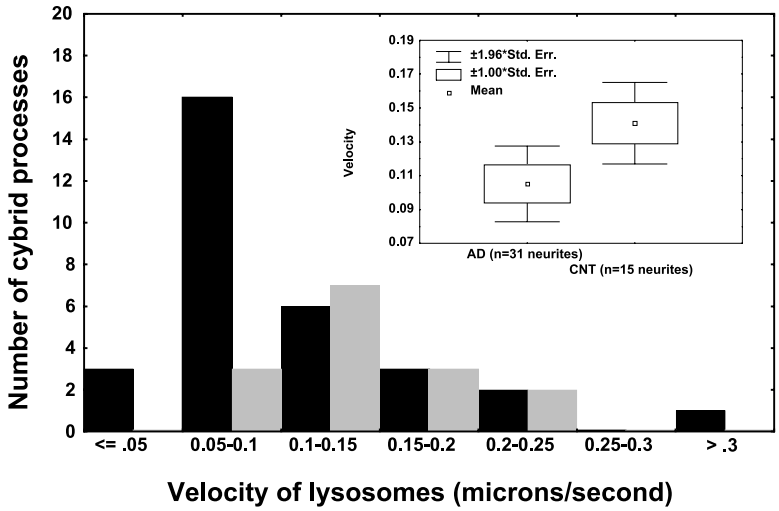

FIG. 4. The histogram shows that the average velocity of lysosome movement in the processes of 31 dAD cybrid cells (black bars) was significantly reduced ($p < 0.05$) when compared with movement of lysosomes in 15 processes of dCNT cybrid cells (gray bars) using the *t* test for dependent samples and the Wilcoxon matched pairs test. The same data are shown in the bar and whisker chart (**inset**).

The range in the variance for lysosome velocity in dAD cybrid neurites (0.0032–0.0102, mean 0.0057) was not significantly different from the range in variance in the lysosome velocity in dCNT cybrid neurites (0.0014–0.0049, mean 0.0037) using a two-sample *F* test. The mean lysosome velocity for the six dCNT cell lines examined as 0.141 μm/s with a standard deviation of 0.029 and a SEM of 0.0054. The mean lysosome velocity calculated for the seven dAD cybrid lines examined was 0.105 μm/s with a standard deviation of 0.017 and a SEM of 0.014. The mean dAD ($n = 3$) and dCNT ($n = 3$) lysosome velocities were not significantly different using a *t* test assuming either equal or unequal variance. This suggests that it will be necessary to increase the number of cybrid lines studied to increase the power and achieve significance at the level of cybrid lines rather than cybrid cell processes (shown in Table 1).

DISCUSSION

The major finding of this study is that mitochondria and lysosomes in the neurites of dAD transmitochondrial cybrid cells exhibit a reduced velocity of axonal transport. The transmitochondrial cybrid cell lines generated for these studies are unique because the mtDNA from AD or CNT patient-derived cells (platelets) was transferred into mtDNA-free ρ° human neuroblastoma cells. The resulting cell lines were grown for a minimum of 6 weeks in a selection medium to eliminate incompletely fused cells that have not been repopulated with the donor mtDNA. As cybrid lines share a common nuclear background and identical culture conditions, the phenotypic differences expressed by AD and CNT cybrid lines are an expression of mtDNA differences.

Retinoic acid-differentiated human SH-SY5Y neuroblastoma cells are suitable host cells for this study because they become postmitotic and express cytological features of neurons in culture. The neurites elaborated by dAD and dCNT cybrid cells express neuron-specific β-tubulin, all three neurofilament proteins, the microtubule-associated proteins, MAP-2 and fetal tau, as well as the microtubule motors, kinesin and cytoplasmic dynein (data not shown; 47, 54, 56). The processes of differentiated cybrid cells exhibit the morphology of axons (unbranched with a narrow caliber) or dendrites (tapering and branching). Previous studies have noted that the kinetics of organelle transport in axons and dendrites are essentially the same (28). AD and CNT cybrid neurites express both MAP-2 and tau (data not shown). The failure to segregate tau to the axon is a characteristic of immature neurons (16).

Like other neuronal cells in culture (28), cybrid mitochondrial movement is saltatory and characterized by frequent stops and direction reversals. In contrast, cybrid lysosomal movement in other culture systems tends to be sustained, unidirectional with few stops, and more closely resembles the movement of other vesicular cargo conveyed by axonal transport (1). Both mitochondria and lysosomes follow microtubules as "tracks" for their long-distance excursions into neuronal processes and use members of the kinesin family and cytoplasmic dynein to direct their movement (29). The velocity of lysosome movement was affected slightly more than the velocity of mitochondrial movement in dAD cybrid neurites despite the fact that an age-matched subset consisting of only three AD cybrid lines was compared with a subset of three CNT cybrid lines (Table 1). It will be important to expand the lysosome velocity measurements to include the remainder of the AD and CNT cybrid lines available. Such a differential effect on axonal transport kinetics may be influenced by the specific member of kinesin family each organelle uses to drive anterograde transport (19).

In the neurites of dAD cybrid cells, the velocity of both mitochondrial and lysosomal transport was significantly reduced (Table 1). This observation suggests that one or more components of the transport machinery used by both organelles are compromised by the presence of dysfunctional mitochondria expressing mtDNA from AD patients. AD cybrids exhibit increased levels of ROS, elevated basal cytosolic calcium, in-

creased production of Aβ peptides, and a prolonged return to basal calcium levels following stimulation (46, 50). Components of the neuronal cytoskeleton (tubulin, neurofilaments, and tau), as well as the motor proteins, kinesin and cytoplasmic dynein, are highly sensitive to damage from ROS and high levels of calcium (11, 37). Therefore, increased levels of ROS or calcium could compromise the neuronal cytoskeleton and/or motor proteins and their interactions with mitochondria and/or lysosomes. Cash *et al*. (8) suggested that oxidative damage from dysfunctional mitochondria may destabilize microtubules, free tau, and destroy the "track" of axonal transports. In support of this possibility, exposure of rat hippocampal neurons to a clinically relevant concentration of nitric oxide causes a significant reduction in organelle transport and neurite outgrowth (data not shown; 51). Axonal transport can also be transiently inhibited by glutamate exposure, which triggers calcium influx (23). Basal calcium levels and recovery of calcium following influx were compromised in proliferating AD cybrids (46). Altered calcium homeostasis may therefore play a role in the reduction of axonal transport of mitochondria seen in dAD cybrids. Direct application of Aβ42 peptides has also been shown to inhibit fast axonal transport in sciatic nerve (23). In cultured hippocampal neurons, Aβ application resulted in an irreversible inhibition of active transport (20). Although we have not determined the level of Aβ expression in differentiated cybrids, undifferentiated AD cybrids generate increased levels of Aβ peptides (24).

The mitochondria in dAD cybrid neurites were significantly longer and more thread-like than the mitochondria in dCNT cybrid neurites. Bertoni-Freddari *et al.* (4) found that enlargement of mitochondrial size is inversely correlated with CO activity. This is consistent with our measurement of reduced CO activity in undifferentiated AD cybrid lines (50). Varadi *et al.* (55) disrupted cytoplasmic dynein function with the p50 dynactin subunit. This manipulation unexpectedly caused the formation of long, interconnected mitochondria. They speculated that cytoplasmic dynein is important for the correct mitochondrial targeting of molecules such as dynamin-related protein, a protein involved in mitochondrial fission. They further suggest that a shift between mitochondrial fission and fusion by interference with dynein-related protein localization would result in longer, interconnected mitochondria. In dAD cybrid neurites, long mitochondria appeared to have a reduced velocity of transport compared with short mitochondria in the same neurite. This could reflect a reduced ability of the motor proteins to remain attached to the microtubule, as suggested by Welte (57), or a reduced ability of mitochondria to reattach to a new microtubule after reaching the end of the previous microtubule.

Studies by Mandelkow *et al.* (31) have also shed light on the role that microtubules and tau may play in the loss of axonal transport in AD. By overexpressing labeled tau, they were able to show that tau interferes with the relationship between microtubules and anterograde motors like kinesin. This results in a gradual redistribution of cellular organelles like mitochondria out of the neurites and back to the perinuclear region, energy loss, increased susceptibility to ROS, and neuritic retraction. In contrast, the mitochondria and lysosomes in dAD cybrids continue to occupy neurites. The mechanism of reduced organelle movement in dAD cybrid neurites appears to be different from the effect achieved by overexpressing tau. The velocity of both lysosomes and mitochondria was reduced, but not eliminated. The reduction in run length and excursion length suggests that the organelles were not able to remain attached to microtubules as long as in dCNT neurites. This could be a consequence of a reduced ability of kinesin or cytoplasmic dynein to remain attached to microtubules, or due to damage to the microtubules themselves. Further studies will be directed at understanding how levels of ROS, Aβ peptides, and calcium alter the integrity and function of microtubules and motor proteins and how these changes alter organelle movements in differentiated cybrid neurites.

Perspectives

The association between mitochondrial ETC dysfunction and AD was made over a decade ago (for review, see 49). Recent articles have increased our understanding of the critical role that mitochondrial ETC dysfunction and related increases in the generation of ROS play in AD pathogenesis (27). Mutations and altered processing of the APP to yield Aβ peptides generate the plaques that are diagnostic for AD. It is now known that APP contains a mitochondrial targeting signal (2) and that mitochondrial dysfunction is directly linked to Aβ peptides by the Aβ-binding alcohol dehydrogenase (30). Finally, components of the γ-secretase that participate in the generation of Aβ are present in the mitochondrion (17). The results of our study showed that mtDNA derived from AD patients and expressed in an mtDNA-free ρ° neuroblastoma cell resulted in a disruption of the axonal transport of both mitochondria and lysosomes. In 1967, Suzuki and Terry (48) reported that AD is characterized by substantial axonal transport abnormalities. Synaptic terminals and axons are dependent on axonal transport to sustain their function, and the best correlate of cognitive decline in AD is synaptic loss (27). This study and the others cited above clearly suggest that mitochondrial ETC dysfunction, whether due to mtDNA mutation or the effects of Aβ peptide generation, can result in reduced axonal transport in AD. Reduced axonal transport puts synaptic terminals at risk due to a loss of vital constituents and may result in the terminal degeneration seen early in AD pathogenesis. Further studies are needed to clarify how these processes interact to generate neuronal dysfunction and death in AD.

ACKNOWLEDGMENTS

This research was supported by NIH grant AG14373. We are grateful to Jatanna Rigsby for technical assistance and to James P. Bennett, Jr. and other members of the Center for the Study of Neurodegenerative Diseases at UVA for insightful comments.

ABBREVIATIONS

Aβ, β-amyloid; AD, Alzheimer's disease; APP, amyloid precursor protein; CNT, control; CO, cytochrome *c* oxidase; cybrid, cytoplasmic hybrid; dAD, differentiated AD cybrid; dCNT, differentiated control cybrid; ETC, electron transport chain; LysoRed, LysoTracker Red; mtDNA, mitochondrial DNA; MTRed, MitoTracker CMXROS; ρ° cell, mitochon-

drial DNA-free cell; ROS, reactive oxygen species; SEM, standard error of the mean.

REFERENCES

1. Aihara Y, Inoue T, Tashiro T, Okamoto K, Komiya Y, and Mikoshiba K. Movement of endoplasmic reticulum in the living axon is distinct from other membranous vesicles in its rate, form, and sensitivity to microtubule inhibitors. *J Neurosci Res* 65: 236–246, 2001.
2. Anandatheerthavarada HK, Biswas G, Robin MA, and Avadhani NG. Mitochondrial targeting and a novel transmembrane arrest of Alzheimer's amyloid precursor protein impairs mitochondrial function in neuronal cells. *J Cell Biol* 161: 41–54, 2003.
3. Bendiske J and Bahr BA. Lysosomal activation is a compensatory response against protein accumulation and associated synaptopathogenesis—an approach for slowing Alzheimer disease? *J Neuropathol Exp Neurol* 62: 451–463, 2003.
4. Bertoni-Freddari C, Fattoretti P, Paoloni R, Caselli U, Giorgetti B, and Solazzi M. Inverse correlation between mitochondrial size and metabolic competence: a quantitative cytochemical study of cytochrome oxidase activity. *Naturwissenschaften* 90: 68–71, 2003.
5. Brown A. Axonal transport of membranous and nonmembranous cargoes: a unified perspective. *J Cell Biol* 160: 817–821, 2003.
6. Buxbaum JD, Thinakaran G, Koliatsos V, O'Callahan J, Slunt HH, Price DL, and Sisodia SS. Alzheimer amyloid protein precursor in the rat hippocampus: transport and processing through the perforant path. *J Neurosci* 18: 9629–9637, 1998.
7. Cardoso SM, Proenca MT, Santos S, Santana I, and Oliveira CR. Cytochrome *c* oxidase is decreased in Alzheimer's disease platelets. *Neurobiol Aging* 25: 105–110, 2004.
8. Cash AD, Aliev G, Siedlak SL, Nunomura A, Fujioka H, Zhu X, Raina AK, Vinters HV, Tabaton M, Johnson AB, Paula-Barbosa M, Avila J, Jones PK, Castellani RJ, Smith MA, and Perry G. Microtubule reduction in Alzheimer's disease and aging is independent of tau filament formation. *Am J Pathol* 162: 1623–1627, 2003.
9. Cataldo AM, Barnett JL, Berman SA, Li J, Quarless S, Bursztajn S, Lippa C, and Nixon RA. Gene expression and cellular content of cathepsin D in Alzheimer's disease brain: evidence for early up-regulation of the endosomal-lysosomal system. *Neuron* 14: 671–680, 1995.
10. Coleman PD and Yao PJ. Synaptic slaughter in Alzheimer's disease. *Neurobiol Aging* 24: 1023–1027, 2003.
11. Cookson MR, Thatcher NM, Ince PG, and Shaw PJ. Selective loss of neurofilament proteins after exposure of differentiated human IMR-32 neuroblastoma cells to oxidative stress. *Brain Res* 738: 162–166, 1996.
12. Coskun PE, Beal MF, and Wallace DC. Alzheimer's brains harbor somatic mtDNA control-region mutations that suppress mitochondrial transcription and replication. *Proc Natl Acad Sci U S A* 101: 10726–10731, 2004.
13. Crosby AH. Disruption of cellular transport: a common cause of neurodegeneration? *Lancet Neurol* 2: 311–316, 2003.
14. Dai J, Buijs RM, Kamphorst W, and Swaab DF. Impaired axonal transport of cortical neurons in Alzheimer's disease is associated with neuropathological changes. *Brain Res* 948: 138–144, 2002.
15. Di Luca M, Colciaghi F, Pastorino L, Borroni B, Padovani A, and Cattabeni F. Platelets as a peripheral district where to study pathogenetic mechanisms of Alzheimer disease: the case of amyloid precursor protein. *Eur J Pharmacol* 405: 277–283, 2000.
16. Dotti CG, Banker GA, and Binder LI. The expression and distribution of the microtubule-associated proteins tau and microtubule-associated protein 2 in hippocampal neurons in the rat in situ and in cell culture. *Neuroscience* 23: 121–130, 1987.
17. Hansson CA, Frykman S, Farmery MR, Tjernberg LO, Nilsberth C, Pursglove SE, Ito A, Winblad B, Cowburn RF, Thyberg J, and Ankarcrona M. Nicastrin, presenilin, APH-1, and PEN-2 form active γ-secretase complexes in mitochondria. *J Biol Chem* 279: 51654–51660, 2004.
18. Hirai K, Aliev G, Nunomura A, Fujioka H, Russell RL, Atwood CS, Johnson AB, Kress Y, Vinters HV, Tabaton M, Shimohama S, Cash AD, Siedlak SL, Harris PL, Jones PK, Petersen RB, Perry G, and Smith MA. Mitochondrial abnormalities in Alzheimer's disease. *J Neurosci* 21: 3017–3023, 2001.
19. Hirokawa N and Takemura R. Kinesin superfamily proteins and their various functions and dynamics. *Exp Cell Res* 301: 50–59, 2004.
20. Hiruma H, Katakura T, Takahashi S, Ichikawa T, and Kawakami T. Glutamate and amyloid beta-protein rapidly inhibit fast axonal transport in cultured rat hippocampal neurons by different mechanisms. *J Neurosci* 23: 8967–8977, 2003.
21. Hollenbeck PJ. Products of endocytosis and autophagy are retrieved from axons by regulated retrograde organelle transport. *J Cell Biol* 121: 305–315, 1993.
22. Huang HM, Martins R, Gandy S, Etcheberrigaray R, Ito E, Alkon DL, Blass J, and Gibson G. Use of cultured fibroblasts in elucidating the pathophysiology and diagnosis of Alzheimer's disease. *Ann N Y Acad Sci* 747: 225–244, 1994.
23. Kasa P, Papp H, Kovacs I, Forgon M, Penke B, and Yamaguchi H. Human amyloid-beta1–42 applied in vivo inhibits the fast axonal transport of proteins in the sciatic nerve of rat. *Neurosci Lett* 278: 117–119, 2000.
24. Khan SM, Cassarino DS, Abramova NN, Keeney PM, Borland MK, Trimmer PA, Krebs CT, Bennett JC, Parks JK, Swerdlow RH, Parker WD Jr, and Bennett JP Jr. Alzheimer's disease cybrids replicate beta-amyloid abnormalities through cell death pathways. *Ann Neurol* 48: 148–155, 2000.
25. King MP and Attardi G. Human cells lacking mtDNA: repopulation with exogenous mitochondria by complementation. *Science* 246: 500–503, 1989.
26. Lambert MP, Stevens G, Sabo S, Barber K, Wang G, Wade W, Krafft G, Snyder S, Holzman TF, and Klein WL. Beta/A4-evoked degeneration of differentiated SH-SY5Y human neuroblastoma cells. *J Neurosci Res* 39: 377–385, 1994.
27. Lee HG, Moreira PI, Zhu X, Smith MA, and Perry G. Staying connected: synapses in Alzheimer disease. *Am J Pathol* 165: 1461–1464, 2004.
28. Ligon LA and Steward O. Movement of mitochondria in the axons and dendrites of cultured hippocampal neurons. *J Comp Neurol* 427: 340–350, 2000.

29. Ligon LA and Steward O. Role of microtubules and actin filaments in the movement of mitochondria in the axons and dendrites of cultured hippocampal neurons. *J Comp Neurol* 427: 351–361, 2000.
30. Lustbader JW, Cirilli M, Lin C, Xu HW, Takuma K, Wang N, Caspersen C, Chen X, Pollak S, Chaney M, Trinchese F, Liu S, Gunn-Moore F, Lue LF, Walker DG, Kuppusamy P, Zewier ZL, Arancio O, Stern D, Yan SS, and Wu H. ABAD directly links Aβ to mitochondrial toxicity in Alzheimer's disease. *Science* 304: 448–452, 2004.
31. Mandelkow EM, Stamer K, Vogel R, Thies E, and Mandelkow E. Clogging of axons by tau, inhibition of axonal traffic and starvation of synapses. *Neurobiol Aging* 24: 1079–1085, 2003.
32. Marino G and Lopez-Otin C. Autophagy: molecular mechanisms, physiological functions and relevance in human pathology. *Cell Mol Life Sci* 61: 1439–1454, 2004.
33. Masliah E, Mallory M, Alford M, DeTeresa R, Hansen LA, McKeel DW Jr, and Morris JC. Altered expression of synaptic proteins occurs early during progression of Alzheimer's disease. *Neurology* 56: 127–129, 2001.
34. Mattson MP. Pathways towards and away from Alzheimer's disease. *Nature* 430: 631–639, 2004.
35. Mattson MP and Liu D. Mitochondrial potassium channels and uncoupling proteins in synaptic plasticity and neuronal cell death. *Biochem Biophys Res Commun* 304: 539–549, 2003.
36. Mattson MP and Partin J. Evidence for mitochondrial control of neuronal polarity. *J Neurosci Res* 56: 8–20, 1999.
37. Mattson MP, Engle MG, and Rychlik B. Effects of elevated intracellular calcium levels on the cytoskeleton and tau in cultured human cortical neurons. *Mol Chem Neuropathol* 15: 117–142, 1991.
38. Miller SW, Trimmer PA, Parker WD Jr, and Davis RE. Creation and characterization of mitochondrial DNA-depleted cell lines with "neuronal-like" properties. *J Neurochem* 67: 1897–1907, 1996.
39. Mufson EJ, Kroin JS, Sendera TJ, and Sobreviela T. Distribution and retrograde transport of trophic factors in the central nervous system: functional implications for the treatment of neurodegenerative diseases. *Prog Neurobiol* 57: 451–484, 1999.
40. Muslimov IA, Titmus M, Koenig E, and Tiedge H. Transport of neuronal BC1 RNA in Mauthner axons. *J Neurosci* 22: 4293–4301, 2002.
41. Parker WD Jr, Mahr NJ, Filley CM, Parks JK, Hughes D, Young DA, and Cullum CM. Reduced platelet cytochrome *c* oxidase activity in Alzheimer's disease. *Neurology* 44: 1086–1090, 1994.
42. Pascale A and Etcheberrigaray R. Calcium alterations in Alzheimer's disease: pathophysiology, models and therapeutic opportunities. *Pharmacol Res* 39: 81–88, 1999.
43. Praprotnik D, Smith MA, Richey PL, Vinters HV, and Perry G. Filament heterogeneity within the dystrophic neurites of senile plaques suggests blockage of fast axonal transport in Alzheimer's disease. *Acta Neuropathol (Berl)* 91: 226–235, 1996.
44. Ray K, Perez SE, Yang Z, Xu J, Ritchings BW, Steller H, and Goldstein LS. Kinesin-II is required for axonal transport of choline acetyltransferase in *Drosophila*. *J Cell Biol* 147: 507–518, 1999.
45. Saraiva AA, Borges MM, Madeira MD, Tavares MA, and Paula-Barbosa MM. Mitochondrial abnormalities in cortical dendrites from patients with Alzheimer's disease. *J Submicrosc Cytol* 17: 459–464, 1985.
46. Sheehan JP, Swerdlow RH, Miller SW, Davis RE, Parks JK, Parker WD, and Tuttle JB. Calcium homeostasis and reactive oxygen species production in cells transformed by mitochondria from individuals with sporadic Alzheimer's disease. *J Neurosci* 17: 4612–4622, 1997.
47. Smith CJ, Anderton BH, Davis DR, and Gallo JM. Tau isoform expression and phosphorylation state during differentiation of cultured neuronal cells. *FEBS Lett* 375: 243–248, 1995.
48. Suzuki K and Terry RD. Fine structural localization of acid phosphatase in senile plaques in Alzheimer's presenile dementia. *Acta Neuropathol (Berl)* 8: 276–284, 1967.
49. Swerdlow RH and Kish SJ. Mitochondria in Alzheimer's disease. *Int Rev Neurobiol* 53: 341–385, 2002.
50. Swerdlow RH, Parks JK, Cassarino DS, Maguire DJ, Maguire RS, Bennett JP Jr, Davis RE, and Parker WD Jr. Cybrids in Alzheimer's disease: a cellular model of the disease? *Neurology* 49: 918–925, 1997.
51. Trimm KR and Rehder V. Nitric oxide acts as a slow-down and search signal in developing neurites. *Eur J Neurosci* 19: 809–818, 2004.
52. Trimmer PA, Swerdlow RH, Parks JK, Keeney P, Bennett JP Jr, Miller SW, Davis RE, and Parker WD Jr. Abnormal mitochondrial morphology in sporadic Parkinson's and Alzheimer's disease cybrid cell lines. *Exp Neurol* 162: 37–50, 2000.
53. Trimmer PA, Keeney PM, Borland MK, Simon FA, Almeida J, Swerdlow RH, Parks JP, Parker WD Jr, and Bennett JP Jr. Mitochondrial abnormalities in cybrid cell models of sporadic Alzheimer's disease worsen with passage in culture. *Neurobiol Dis* 15: 29–39, 2004.
54. Uberti D, Rizzini C, Spano PF, and Memo M. Characterization of tau proteins in human neuroblastoma SH-SY5Y cell line. *Neurosci Lett* 235: 149–153, 1997.
55. Varadi A, Johnson-Cadwell LI, Cirulli V, Yoon Y, Allan VJ, and Rutter GA. Cytoplasmic dynein regulates the subcellular distribution of mitochondria by controlling the recruitment of the fission factor dynamin-related protein-1. *J Cell Sci* 117: 4389–4400, 2004.
56. Vignali G, Niclas J, Sprocati MT, Vale RD, Sirtori C, and Navone F. Differential expression of ubiquitous and neuronal kinesin heavy chains during differentiation of human neuroblastoma and PC12 cells. *Eur J Neurosci* 8: 536–544, 1996.
57. Welte MA. Bidirectional transport along microtubules. *Curr Biol* 14: R525–R537, 2004.

Address reprint requests to:
Patricia A. Trimmer, Ph.D.
Department of Neurology
P.O. Box 800394
Hospital Drive
University of Virginia
Charlottesville, VA 22908

E-mail: pat5q@virginia.edu

Received for publication February 22, 2005; accepted March 8, 2005.

This article has been cited by:

1. Sónia C. Correia, Renato X. Santos, Susana Cardoso, Cristina Carvalho, Emanuel Candeias, Ana I. Duarte, Ana I. Plácido, Maria S. Santos, Paula I. Moreira. 2012. Alzheimer disease as a vascular disorder: Where do mitochondria fit?. *Experimental Gerontology* . [CrossRef]
2. Russell H. Swerdlow . 2012. Mitochondria and Cell Bioenergetics: Increasingly Recognized Components and a Possible Etiologic Cause of Alzheimer's Disease. *Antioxidants & Redox Signaling* **16**:12, 1434-1455. [Abstract] [Full Text HTML] [Full Text PDF] [Full Text PDF with Links]
3. Ying Zhang, Young Ou, Min Cheng, Habib Shojaei Saadi, Jacob C. Thundathil, Frans A. van der Hoorn. 2012. KLC3 is involved in sperm tail midpiece formation and sperm function. *Developmental Biology* **366**:2, 101-110. [CrossRef]
4. Pinar Coskun, Joanne Wyrembak, Samual E. Schriner, Hsiao-Wen Chen, Christine Marciniack, Frank LaFerla, Douglas C. Wallace. 2012. A mitochondrial etiology of Alzheimer and Parkinson disease. *Biochimica et Biophysica Acta (BBA) - General Subjects* **1820**:5, 553-564. [CrossRef]
5. J. Eva Selfridge, E. Lezi, Jianghua Lu, Russell H. Swerdlow. 2012. Role of mitochondrial homeostasis and dynamics in Alzheimer's disease. *Neurobiology of Disease* . [CrossRef]
6. Diana F. Silva, J. Eva Selfridge, Jianghua Lu, Lezi E, Sandra M. Cardoso, Russell H. SwerdlowMitochondrial Abnormalities in Alzheimer's Disease **64**, 83-126. [CrossRef]
7. Yadong Huang. 2011. Roles of apolipoprotein E4 (ApoE4) in the pathogenesis of Alzheimer's disease: lessons from ApoE mouse models. *Biochemical Society Transactions* **39**:4, 924-932. [CrossRef]
8. Yi Yang, Lin-Qing Feng, Xiao-Xiang Zheng. 2011. Microtubule and kinesin/dynein-dependent, bi-directional transport of autolysosomes in neurites of PC12 cells. *The International Journal of Biochemistry & Cell Biology* **43**:8, 1147-1156. [CrossRef]
9. Yadong Huang. 2010. Mechanisms linking apolipoprotein E isoforms with cardiovascular and neurological diseases. *Current Opinion in Lipidology* **21**:4, 337-345. [CrossRef]
10. Paula M. Keeney , Caitlin K. Quigley , Lisa D. Dunham , Christina M. Papageorge , Shilpa Iyer , Ravindar R. Thomas , Kathleen M. Schwarz , Patricia A. Trimmer , Shaharyar M. Khan , Francisco R. Portell , Kristen E. Bergquist , James P. Bennett , Jr. . 2009. Mitochondrial Gene Therapy Augments Mitochondrial Physiology in a Parkinson's Disease Cell Model. *Human Gene Therapy* **20**:8, 897-907. [Abstract] [Full Text HTML] [Full Text PDF] [Full Text PDF with Links] [Supplemental material]
11. Russell H. Swerdlow. 2007. Mitochondria in cybrids containing mtDNA from persons with mitochondriopathies. *Journal of Neuroscience Research* **85**:15, 3416-3428. [CrossRef]
12. Jose Viña , Ana Lloret , Soraya L. Vallés , Consuelo Borrás , Mari-Carmen Badía , Federico V. Pallardó , Juan Sastre , Maria-Dolores Alonso . 2007. Effect of Gender on Mitochondrial Toxicity of Alzheimer's A# Peptide. *Antioxidants & Redox Signaling* **9**:10, 1677-1690. [Abstract] [Full Text PDF] [Full Text PDF with Links]
13. Michelangelo Mancuso , Fabio Coppedè , Luigi Murri , Gabriele Siciliano . 2007. Mitochondrial Cascade Hypothesis of Alzheimer's Disease: Myth or Reality?. *Antioxidants & Redox Signaling* **9**:10, 1631-1646. [Abstract] [Full Text PDF] [Full Text PDF with Links]
14. Xi Jiang, Jing Li, Lan Ma. 2007. Metabolic enzymes link morphine withdrawal with metabolic disorder. *Cell Research* **17**:9, 741-743. [CrossRef]
15. Lucia Petrozzi, Giulia Ricci, Noemi J. Giglioli, Gabriele Siciliano, Michelangelo Mancuso. 2007. Mitochondria and Neurodegeneration. *Bioscience Reports* **27**:1-3, 87-104. [CrossRef]
16. A D Roses, A M Saunders, Y Huang, J Strum, K H Weisgraber, R W Mahley. 2007. Complex disease-associated pharmacogenetics: drug efficacy, drug safety, and confirmation of a pathogenetic hypothesis (Alzheimer's disease). *The Pharmacogenomics Journal* **7**:1, 10-28. [CrossRef]
17. Santina A. Zanelli, Patricia A. Trimmer, Nina J. Solenski. 2006. Nitric oxide impairs mitochondrial movement in cortical neurons during hypoxia. *Journal of Neurochemistry* **97**:3, 724-736. [CrossRef]
18. Yadong Huang, Robert W. Mahley. 2006. Commentary on "Perspective on a pathogenesis and treatment of Alzheimer's disease." Apolipoprotein E and the mitochondrial metabolic hypothesis. *Alzheimer's & Dementia* **2**:2, 71-73. [CrossRef]
19. Janet M. Dubinsky . 2005. CNS Mitochondria in Neurodegenerative Disorders. *Antioxidants & Redox Signaling* **7**:9-10, 1089-1091. [Citation] [Full Text PDF] [Full Text PDF with Links]